# Silicon Photodiodes for Absolute Soft X-ray Radiometry

Jeffrey W. Keister*
SFA, Inc., Bldg 535A, NSLS Dept., Brookhaven National Laboratory, Upton, NY 11973-5000

## ABSTRACT

Absolute spectroscopic photocurrent calibration of detectors in the photon energy range of 50-6000 eV is performed at beamlines U3c and X8a of the National Synchrotron Light Source at Brookhaven National Laboratory. These beamlines are specifically designed to provide high flux over a wide energy range, with particular attention paid to harmonic purity of the monochromatic beam. Examples of optics which enhance the beam purity include transmission foils and grazing-incidence mirrors. The AXUV-100G silicon photodiode available from IRD is used as a reference detector. Its relatively simple design, and the availability of x-ray optical data for silicon and silicon dioxide, permit application of the "self-calibration" method of estimating absolute response, typically to 2% accuracy or better. Characteristics of typical such diodes will be described, including spectroscopic responsivity and models, lot matching, electrical characteristics, visible and infrared light responsivity, and soft x-ray photon-induced damage.

**Keywords:** photodiode, calibration, radiometry, responsivity, beamline, x-ray, synchrotron

## 1. INTRODUCTION

Use of silicon photodiodes in current mode for absolute light power determination has been described at length in the literature [1-3]. Detailed description of the design of the IRD AXUV-100G device can be found elsewhere [1-7]. Essentially the AXUV-100G is an N on P diode with a thin (~5 nm) oxide window and fully depleted active region thickness of 25-50 μm. The oxide is designed to incorporate nitrogen for improved interface quality and added robustness against radiation damage [4, 8-10].

This paper addresses zero-bias current measurement, in contrast with single-photon (counting) methods found in many low-flux applications. While it is possible to perform radiometric calibration on photodiodes in counting mode, that approach is more appropriate at higher energies (where the charge per photon is higher than achievable noise levels) and where sources are weaker (current mode is more suited to synchrotron sources, where photon rates are typically in the $10^9$ photons per second range). In either case, the soft x-ray range (50-1000 eV) presents the additional challenge of detector efficiency being limited by photoelectric absorption in the "dead" or "window" layer, which consists of not only (possibly nitrided) silicon oxide but may also include underlying silicon which is effectively "dead" due to incomplete charge collection in the topmost regions, and may even incorporate other absorbing layers such as nitrogen or metal to make the interface more robust against photon damage or less sensitive to visible light.

These absorbing layers not only attenuate the incoming soft x-rays but may also be some of the hardest parameters to control and maintain in real devices. In other words, significant variability in soft x-ray responsivity can be attributed to small changes both in surface termination process steps and post-processing environment, including soft x-ray illumination. Damage at the silicon-oxide interface, due to high absorbed dose, can have the effect of both increasing "dead" (incomplete charge collection) layer silicon and lowering shunt resistance. On the other hand, variability in silicon dead layer appears even on fresh diodes. In an effort to reduce this variability, responsivity is regularly measured and the data are made available to the vendor.

Herein are described some of the most useful diagnostics available for qualifying commercially-available detectors, and data is provided to illustrate typical performance of IRD AXUV-100G detectors in the soft x-ray range. Performance criteria are developed from our experience at the NSLS U3c and X8a synchrotron beamlines, which as described in the following section, have been optimized for such radiometric characterization.

SPIE Vol. 6689 Solar Physics and Space Weather Instrumentation II (2007)
Paper # 6689-26

*email: jkeister@bnl.gov

## 2. DESCRIPTION OF THE BEAMLINES

Absolute detector responsivity (DC photocurrent) calibration of x-ray detectors in the photon energy range of 50-6000 eV is performed at beamlines U3c and X8a of the National Synchrotron Light Source (NSLS) at Brookhaven National Laboratory [11-15]. Responsivity measurements at beamlines U3c and X8a can typically be compared to model data for a variety of detector types, including photodiode, photoconductor, and photoemission type detectors. Filter transmission and mirror reflectivity are also commonly measured, using the same reference detectors to determine incident and transmitted (reflected) flux. Both beamlines operate under ring-contiguous vacuum. Collimation of the x-ray beam at either end station is typically accomplished by means of a 1/16" diameter circular pinhole.

U3c operates on the NSLS-VUV storage ring (beam energy = 808 MeV), taking approximately 10 mrad from a 1.41 T (1.91 m) bending magnet with critical energy 622 eV. Monochromatic x-rays are provided by either of two gratings in an "extended range grasshopper" (ERG) monochromator [16]. Soft x-rays are refocused by a gold-coated bent cylindrical mirror to maximize flux in the test chamber. Harmonic purity of the x-ray beam is accomplished using both foil x-ray filters and a four-bounce mirror set ("high-order trap") installed on the beamline.

X8a operates on the NSLS-XRAY storage ring (beam energy = 2.8 GeV), taking approximately 4 mrad from a 1.36 T (6.875 m) bending magnet with critical energy 7.1 keV. X-rays are focused to the end station by a nickel-coated bent cylindrical mirror located 7.5 m from the source. Monochromatic x-rays are provided by a dual crystal monochromator using either Si(111) (d = 3.1355 Å) or W/Si (d = 25 Å) Bragg dispersion elements. Harmonic purity of the x-ray beam is accomplished using foil x-ray filters installed on the beamline, in addition to the upstream mirror which provides a high-energy cutoff near 5.9 keV.

Responsivity of test detectors is measured in comparison to AXUV-100G silicon photodiodes from IRD [7]. Diodes in use as reference detectors are specified to have maximum 50 nm silicon dead layer and minimum 500 megaohm shunt resistance. Active layer thickness is typically 25 μm. Absolute responsivity of the reference diode is determined using the "self-calibration" method of Krumrey and Tegeler [17, 18]; optical constants required for this approach are taken from several references [19-22]. Spectroscopic responsivity of the reference diodes installed at the beamlines ranges from 0.15 to 0.27 A/W in the range of 50-6000 eV and is typically measured at these beamlines at specific energies with an absolute radiometric accuracy of 2-5%.

Beamline features most critical to the successful execution of radiometric calibrations at this accuracy range include broad energy range (50-6000 eV), high harmonic purity (95-99%), reasonable flux (sufficient for 1 nA or greater silicon diode current), and positioning accuracy of 0.5 mm or better.

Presently, the principle scientific motivation for the existence of the NSLS U3c and X8a beamlines is high temperature fusion plasma research occurring at several high-profile national sites, including the NIF and Omega high-power laser facilities, and the Z-pinch machine at Sandia National Laboratory [23-31]. These experiments rely critically on accurately calibrated x-ray radiometric diagnostics (detectors, filters, mirrors, etc.). Beamline operations funding is provided on behalf of those and related programs by National Security Technologies, LLC.

## 3. MEASUREMENTS

### 3.1 Electrical performance

The electrical performance of the photodiode must be measured in a dark environment. This is accomplished by a light-tight and electrically shielded box with isolated feedthroughs for anode and cathode. Care is taken to prevent any part of the diode from touching the box wall (chassis ground). Based on our observations, no significant variation in ultimate electrical performance has been found using different gases to fill the dark box, such as air, dry air, inert gas, or vacuum; therefore air is typically used for bench tests and vacuum is typically used for diodes installed to the beamline endstations. With no bias applied, the diode is connected to an isolated ammeter using triax cable (center HI conductor to anode, inner LO shield to cathode, and neither diode lead connected to the ammeter chassis, dark box chassis, or triax cable outer shield). This configuration yields the dark current. The minimum value for dark current we have found so far is roughly 50 fA; this is believed to be limited by electrical leakage in the cable and its connectors. Our acceptance

criterion for dark current for diodes operating on the beamline is magnitude of 1 pA or less (occasionally negative dark current is seen. Larger negative current is associated with low shunt resistance of a damaged detector.).

Although it is a quick test, we have found that dark current itself is not a reliable measure of diode health, since it depends upon the diode's shunt resistance, the performance of the ammeter used, and the electrical environment where the diode is installed. Instead of dark current, we measure diode electrical performance chiefly in terms of shunt resistance. Both positive and negative 10 mV bias is applied using a calibrated bipolar voltage source and in each case the shunt resistance is estimated as the ratio of the bias to the observed current. For this test, the ammeter input HI is cabled to the diode's anode, the ammeter input LO is cabled to the source output LO, and the source output HI is cabled to the diode's cathode. This provides the applied bias in series with the current measurement. Under negative bias, a negative current should be measured, so that both bias directions yield roughly the same shunt resistance value. The final quoted value is taken as the average of the two shunt resistances measured with positive and negative applied bias, and typically the two values do not disagree by more than 10%. Typical shunt resistance values for new IRD AXUV-100G diodes range from 20 MΩ to 4 GΩ. Minimum acceptable value for us is 500 MΩ; this requirement is driven primarily by known limitations of ammeters for low current measurements in low load resistance situations.

### 3.2 Visible and infrared light responsivity

The AXUV-100G, being essentially windowless (having no thick window added), is intrinsically sensitive to visible and infrared light. Soft x-ray measurements, therefore, must be made with care taken to eliminate ambient light which may corrupt the diode response. At the U3c beamline, the chamber is kept dark and windows are covered, so that only monochromatic soft x-rays contribute to the measured signal. Also, foil filters are used at each beamline to help block scattered visible light from upstream parts of the beamline from entering the test chamber.

Likewise, in field measurements, foils or films may be integrated with a detector to block visible light. The foil's impact on the detector's x-ray responsivity can be minimized by using the thinnest possible foils, or even layering flash coatings of inert metals like aluminum directly onto the detector. However, the effect this has on the x-ray responsivity of the detector-foil system should still be explicitly considered, since even the thinnest films will block soft x-rays.

In fact, foils can be used as bandpass filters in the soft x-ray range [23, 24, 30, 32]; multilayer coatings may also be considered [33, 34]. For our application, the simpler "nude" diodes are best suited for radiometric measurements, as long as the visible light is kept out of the system by the methods described above (operating dark current is kept below 1 pA).

Internal quantum efficiency (IQE) measurements have been made in the UV range (160-320 nm, 3.9-7.7 eV) [4, 6]. These measurements are intended to determine the charge collection efficiency of the underlying silicon by measuring the total responsivity of the device and taking into account the oxide absorbance using known optical constants. It should be pointed out that for a perfect device, the IQE will exceed unity for photon energies in excess of the mean electron-hole-pair production energy *w*, which has a value of 3.66 eV[19]. Ideally, above 3.66 eV (wavelength below 340 nm), the IQE should be equal to the photon energy divided by *w*. Near this energy is a delimiter between two regimes where either single or multiple electrons can be released per photon; also the silicon attenuation length is different in the two energy ranges. Therefore, since there is no well-established correlation between performance in the UV range to performance in the soft x-ray range, it is desirable to extend responsivity testing to the soft x-ray range where the devices will be used.

### 3.3 Soft x-ray responsivity

The most important measurement of the diode's performance is its responsivity. Ideally it is measured with respect to a calorimetric standard such as an absolute cryogenic radiometer; several groups have adopted this methodology with good success in various energy ranges [35-38]. However, it has been shown that in the absence of such an instrument, reasonably accurate results (2-5%) can be achieved using a "self calibrated" silicon diode as a standard detector [17, 18]. The self-calibration method relies on a physical model of the diode which essentially consists of a model function, reference optical data, and fitting parameters which correspond to various attributes of the diode such as layer thickness and collection efficiency. The sources of error for the self-calibration include optical reference data, beamline out-of-band light, measured signal error, error in the bulk silicon responsivity, diode spatial uniformity, reflectivity losses, and collection of charge from the oxide layer. Reflectivity is estimated from the available optical databases as contributing

less than 1% error in the self-calibration for photon energies at or above 50 eV [20, 21]. Similarly, the importance of charge collection from oxide absorption has been shown to be negligible above 40 or 50 eV [3, 39, 40].

In the interest of clarity, the model we use is now described in detail. The responsivity function used is the following:

$$S = \frac{1}{w}\left[\left(e^{-t_C/\lambda_C} e^{-t_{ox}/\lambda_{ox}} e^{-t_{ds}/\lambda_{Si}}\right)\left(1 - e^{-t_{as}/\lambda_{Si}}\right) + \sigma_s\left(e^{-t_C/\lambda_C} e^{-t_{ox}/\lambda_{ox}}\right)\left(1 - e^{-t_{ds}/\lambda_{Si}}\right)\right] \quad (1)$$

where S is the energy-dependent responsivity of the silicon diode, which consists of the following layers: carbon contamination overlayer, silicon oxide, "dead" layer silicon (which has fixed probability $\sigma_s$ of converting absorbed light into measured photocurrent), and active layer silicon. The thicknesses and photoabsorption attenuation lengths for each of these materials are given by $t$ and $\lambda$, for the materials specified *C* (carbon), *ox* (oxide), *ds* (dead layer silicon), *Si* (silicon), and *as* (active layer silicon). The value *w* is the average electron-hole pair production energy at room temperature (3.66 ± 0.03 eV) [19]. This value, as measured for soft x-rays, is consistent with that measured for hard x-rays as early as 1968 (3.67 ± 0.02 eV) [41]. It is therefore a constant, although it is still not known with precision better than ~1% at room temperature. This model can be state verbally as: "bulk responsivity of silicon over the thickness of the active layer, attenuated by the absorption of the combined carbon, oxide and dead-layer silicon window overlayers, plus some fraction of the bulk silicon responsivity over the thickness of the "dead" silicon layer, attenuated by the absorption of the combined carbon and oxide window overlayers."

The attenuation lengths $\lambda$ used in the calculation of responsivity come from CXRO [20, 21], with the exception of the data for $SiO_2$ below 150 eV for which [22] is used. Although the K edges are known to be quite sharp, the silicon L edge is more complex in $SiO_2$ [9, 10, 42]. The optical data of reference [22] is therefore used, since it is measured from a real system and shows qualitative similarity to our observations of the silicon photodiode (e.g. sharp absorption near 109 eV). The materials properties (molecular weight and density) for silicon, silicon oxide and carbon are taken to be 28.0855 g/mol, 2.33 g/cc, 50.0843 g/mol, 2.2 g/cc, 12.0107 g/mol and 2.26 g/cc, respectively. The optical data used are shown in Figure 1.

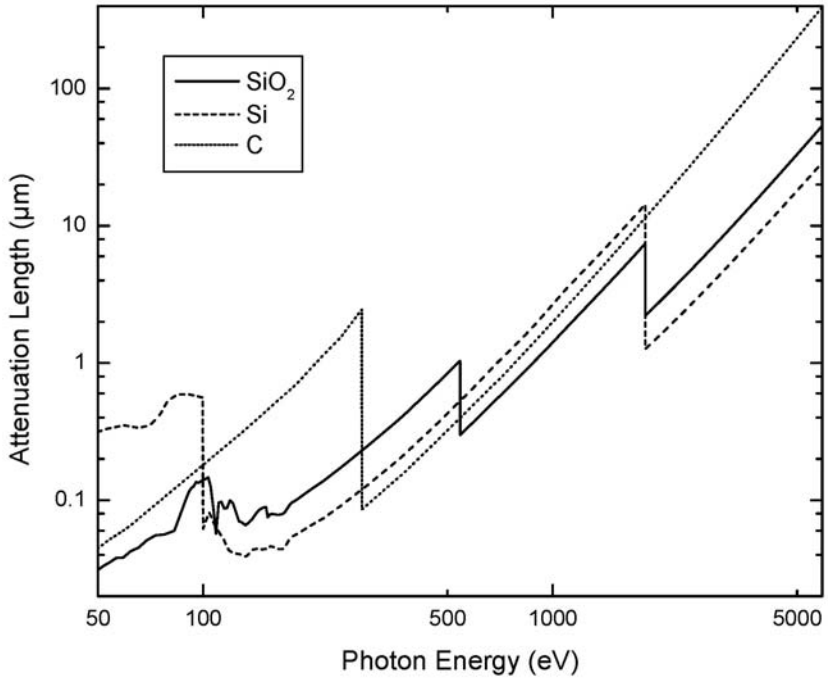


Fig. 1. Photoelectric absorption attenuation lengths used to calculate soft x-ray responsivity from the model and parameters described in the text. The sources of these data are references [20-22].

In the self-calibration procedure, the flux-normalized signal (proportional to S) is measured at normal incidence and again at 60 degrees from normal (thus effectively doubling film thicknesses), across a wide range of photon energies. The ratio of these two signals (what we call A60) is therefore also the ratio of S with single and double thicknesses, and all parameters but *w* can be effectively extracted from a fit of such data.

For illustrative purposes, self-calibration data from beamline U3c is shown with both responsivity ratio (fit) and corresponding responsivity model curves in Figure 2.

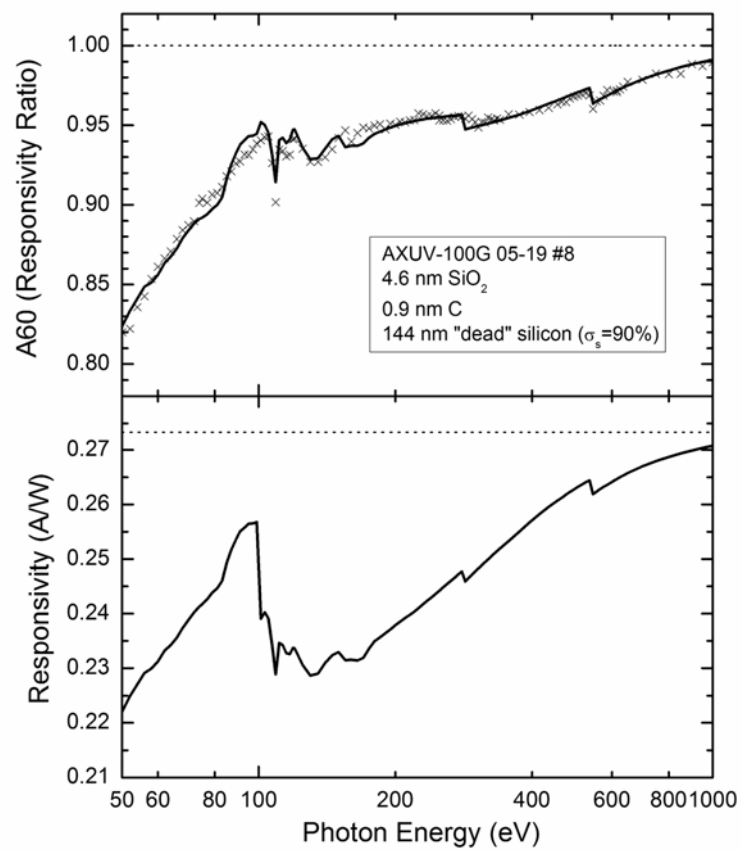


Fig. 2. Example responsivity ratio (self-calibration) data, with corresponding fit, parameters, and responsivity curve for an AXUV-100G photodiode. Reference lines are added for A60=1 and S=1/*w* as described in the text.

Since the transmission of the active layer is negligible (less than 1% for thicknesses above 15 μm) at photon energies below 1 keV, only the window material affects the responsivity in that range. Here, the soft x-ray responsivity is determined by the window layer attenuation, and, as long as there is no silicon dead layer, S is proportional to A60. Near 1 keV, the diode is volumetric, as the window becomes practically transparent while the active layer remains opaque. This corresponds to where A60 is 1, and the diode has the physically maximum possible responsivity S of 1/*w* (0.273 A/W); this occurs near 1 keV and 3 keV for most diodes we have studied so far. At higher energies, the diode efficiency is limited by transmission of the active layer. In the high-energy limit, the attenuation length becomes many times the active layer thickness, and the A60 value asymptotically approaches 2 as S approaches zero. At beamline U3c, measurements are made at photon energies between 50 eV and 1 keV; at beamline X8a, the data are measured at energies between 1 keV and 6 keV. The 1 keV breakpoint between the beamlines acts as a convenient delimiter between window-layer absorption (at low energy) and active-layer transmission (at high energy) modes of reduction of the bulk silicon responsivity.

For photon energies above 1 keV, the self-calibration consists simply of the determination of the active layer thickness. In practice, we have found that this value can be consistently controlled (by the vendor) and determined (at the beamline) to within 1 μm accuracy. This translates to < 0.5% error in the responsivity for photon energies between 1 and 5 keV for the thinnest known (25 μm) version of the AXUV-100G diode. Thus, with the design thickness known,

we can in principle accurately predict responsivity for the higher energies. However, we don't always know the design thickness, and it is subject to change between lots (25-50 μm). Luckily, the active layer thickness does not change over the diode's lifetime. So, in practice, we measure this parameter less often, and favor standardization of the active layer thickness to a single possible value for the AXUV-100G.

The measurements we are most concerned with in this paper are for the lower energies (50-1000 eV), where there is more variability in the diode responsivity, and more physical parameters affecting it. The parameters used to fit the model to real data in this range include oxide thickness (typically 5 ± 1 nm), carbon dead layer thickness (typically 1 ± 0.3 nm), silicon dead layer thickness (variable, 0-200 nm), and silicon dead layer collection efficiency (70-100% for those diodes with significant dead layer thickness, can be 0% otherwise).

Once a reference is established, responsivity measurements for additional diodes are made by transfer calibration. If needed, the same responsivity model which we used for self-calibration can be used to estimate parameter values from the measured responsivity curve for a given test photodiode. We have in fact had success identifying parameters which vary most between diodes of various lot and age, but emphasize that the responsivity value itself is more valuable than the model parameter value as a metric of diode performance since it is less subject to interpretation. For example, as discussed in the next section, we have found that 130 eV is the energy at which most variability in diode soft x-ray responsivity occurs. Although this corresponds most closely to the silicon dead layer parameters, we prefer to state the performance criterion in terms of the responsivity itself: 0.234 A/W at 130 eV; this is roughly equivalent to 7% transmission loss to a silicon dead layer of 50 nm thickness and 90% collection efficiency.

Uniformity of the diode's responsivity over its surface is also important for reliable calibration. Typical tests with 1 mm collimation over the 10x10 mm diode area show less than 1% variation on fresh diodes. However, damaged diodes do show localized response degradation (reduced responsivity only in highly illuminated areas). Since soft x-ray illumination is known to cause localized damage to silicon photodiodes, it is important that silicon reference diodes are changed and calibrated every 1-2 years at the beamline.

It should be pointed out that more sophisticated and detailed modeling has been reported by other authors [43, 44]; these approaches achieve better fits by introducing a functional dependence of the collection probability on depth within the silicon layer taken as a whole. The model function we use, although more simplified, provides sufficient flexibility to capture the performance of the diodes to within the absolute responsivity error of the measurements at our beamlines (2-5%). The dead layer we arrive at can be thought of as a "characteristic" or "mean" dead layer with a fixed thickness and collection efficiency, which matches the observed responsivity (in particular, slope of the responsivity curve in the 100-500 eV range depends on the parameter $\sigma_s$).

### 3.4 Variability of fresh photodiodes

Within a given batch of fresh AXUV-100G diodes, responsivity tends to match fairly well (within 2%). However, shunt resistance still varies substantially (20 MΩ – 4 GΩ); there is apparently no correlation between the two measurements for fresh diodes. Between lots, variability in responsivity is also observed. Figure 3 shows measured responsivity curves and model fits for 13 fresh AXUV-100G photodiodes from 6 different lots. The model fits match the measured data within 3%. Fit parameters are given in Table 1, and they are analyzed statistically in Table 2 and Table 3. The parameters which change in the soft x-ray range are chiefly those related to the silicon dead layer. Oxidation appears fairly well controlled, although the trace nitride incorporation might be playing a role here which we cannot quantify.

Comparison of the responsivity curves and their model fits indicate that variability is greatest near 130 eV, and also rises below 70 eV (as shown in Figure 3). The model parameter which correlates most strongly with responsivity at 130 eV is silicon dead layer thickness; the strongest correlation between parameters is between this and the collection efficiency of this layer. The collection efficiency becomes less important as the dead layer becomes thinner, so if the dead layer is thin enough, the collection efficiency can go to zero without significant impact on diode responsivity.

The target performance criterion we have adopted therefore is 0.234 A/W at 130 eV which is roughly equivalent to a window with 5 nm oxide, 1 nm carbon, and 50 nm of "dead" layer (90% efficient) silicon. This cut line divides our sample set roughly in half. It is encouraging to see qualitative agreement with reference [43] which also found collection efficiency near 90% and dead layer silicon thickness in the 100-200 nm range for an AXUV-100G diode. Note that the responsivity also drops at lower energy (< 70 eV) with increasing window thickness, where we also see significant variability in the diode responsivity between diodes of various lots. It may be reasonable, therefore, to expect that where the responsivity is low, photoelectric absorption is high, and so too may be variation in device performance.

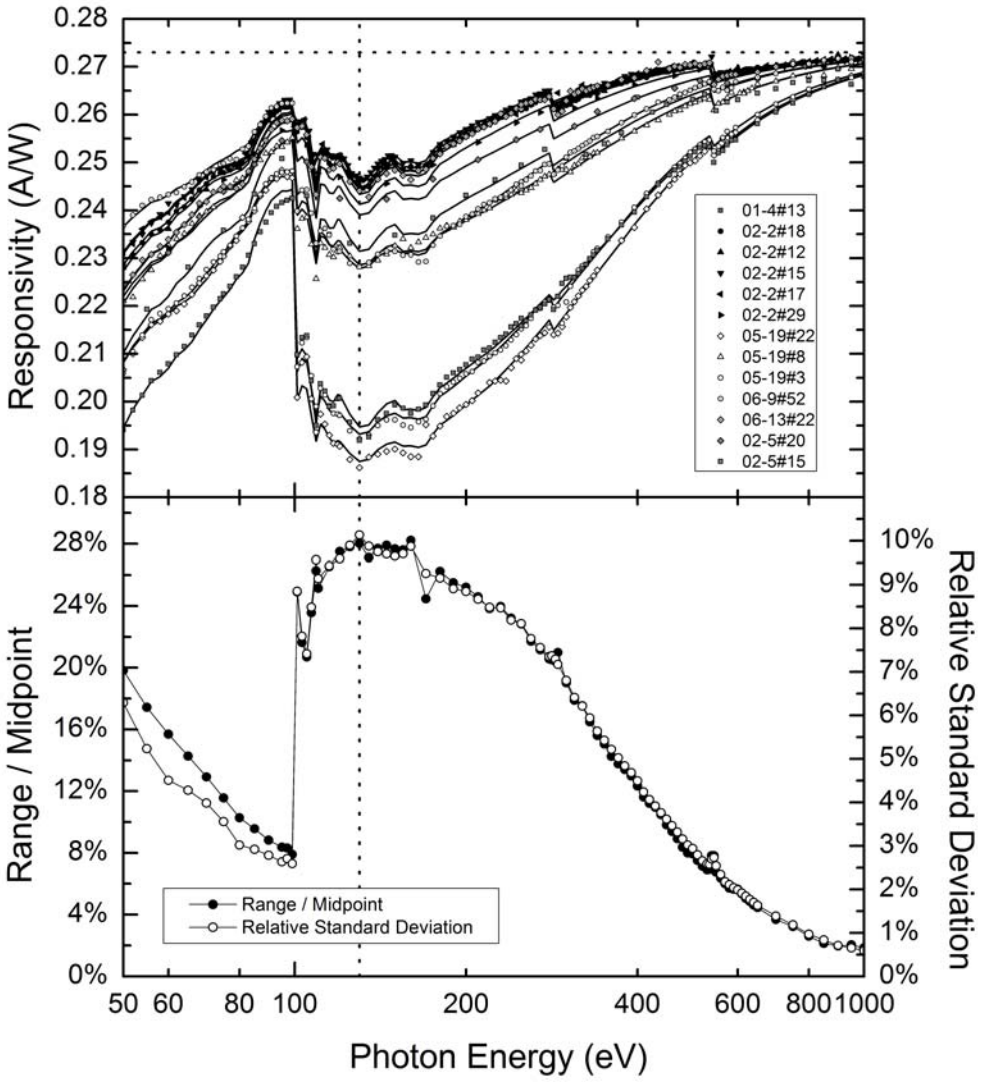


Fig. 3. Measured responsivity curves (50-1000 eV) for AXUV-100G diodes, and variability among the set. The measured responsivity values are shown as symbols, and model functions are drawn through the measured data with fit parameters used as listed in Table 1. The model matches the data to within 3% at each point, whereas the variability among the diodes tested ranges from 1-30% over this photon energy range. Dotted lines are shown at 130 eV and 0.273 A/W for reference.

Responsivities of the diodes at 130 eV are compared in the bar chart of Figure 4. For reference, dotted lines are included in the figure at S = 0.273 A/W (maximum responsivity of 1/*w* if no window is present), S = 0.253 A/W (responsivity with only 5 nm oxide and 1 nm carbon window layers) and S = 0.234 A/W (responsivity with window of 5 nm oxide, 1 nm carbon, and 50 nm dead layer silicon at 90% collection efficiency).

The "typical" responsivity curve of an AXUV-100G photodiode can be estimated as the midpoint (average of minimum and maximum measured responsivity) at each energy, with error bars included to indicate variability. This data is presented in Figure 5.

Table 1. Soft x-ray responsivity performance of several AXUV-100G diodes.

| AXUV-100G diode ID | responsivity at 130 eV (A/W) | oxide layer thickness (nm) | carbon layer thickness (nm) | "dead" layer silicon thickness (nm) | “dead” layer collection efficiency (%) |
|---|---|---|---|---|---|
| 01-4#13 | 0.192 ± 0.008 | 7.2 ± 0.1 | 0.8 ± 0.2 | 168 ± 4 | 79.2 ± 0.1 |
| 02-2#18 | 0.245 ± 0.01 | 4.66 ± 0.04 | 1.03 ± 0.05 | 12 ± 4 | 86 ± 4 |
| 02-2#12 | 0.245 ± 0.01 | 4.9 ± 0.1 | 0.9 ± 0.1 | 5 ± 10 | 68 ± 68 |
| 02-2#15 | 0.247 ± 0.01 | 4.44 ± 0.04 | 0.87 ± 0.06 | 3 ± 5 | 48 ± 80 |
| 02-2#17 | 0.246 ± 0.01 | 4.68 ± 0.04 | 0.58 ± 0.06 | 3 ± 4 | 42 ± 87 |
| 02-2#29 | 0.241 ± 0.01 | 5.1 ± 0.2 | 1.2 ± 0.4 | 28 ± 10 | 92 ± 1 |
| 05-19#22 | 0.186 ± 0.007 | 4.4 ± 0.1 | 1.3 ± 0.2 | 137 ± 3 | 72.7 ± 0.2 |
| 05-19#8 | 0.229 ± 0.009 | 4.6 ± 0.1 | 0.9 ± 0.2 | 144 ± 6 | 89.6 ± 0.5 |
| 05-19#3 | 0.192 ± 0.008 | 4.6 ± 0.1 | 1.5 ± 0.2 | 132 ± 3 | 75.2 ± 0.2 |
| 06-9#52 | 0.228 ± 0.009 | 3.13 ± 0.07 | 0.5 ± 0.1 | 78 ± 3 | 85.5 ± 0.3 |
| 06-13#22 | 0.244 ± 0.01 | 5.70 ± 0.07 | 0.7 ± 0.1 | 1 ± 10 | 30 ± 198 |
| 02-5#20 | 0.239 ± 0.01 | 5.3 ± 0.3 | 1.2 ± 0.6 | 109 ± 25 | 95 ± 1 |
| 02-5#15 | 0.231 ± 0.009 | 6.2 ± 0.3 | 1.5 ± 0.5 | 162 ± 27 | 93.2 ± 0.4 |

Table 2. Statistical analysis of the AXUV-100G diode responsivity parameters of Table 1.

| statistical quantity | responsivity at 130 eV (A/W) | oxide layer thickness (nm) | carbon layer thickness (nm) | "dead" layer silicon thickness (nm) | “dead” layer collection efficiency (%) |
|---|---|---|---|---|---|
| minimum | 0.186 | 3.1 | 0.5 | 1.2 | 30.0 |
| maximum | 0.247 | 7.2 | 1.5 | 168.0 | 95.0 |
| range (maximum-minimum) | 0.061 | 4.1 | 1.0 | 167.0 | 65.0 |
| midpoint (average of minimum and maximum) | 0.217 | 5.2 | 1.0 | 84.5 | 62.5 |
| total variability (range/midpoint) | 28.2% | 78.8% | 100.0% | 197.6% | 104.0% |
| arithmetic mean | 0.228 | 5.0 | 1.0 | 107.8 | 85.4 |
| sample standard deviation (SD) | 0.023 | 1.0 | 0.3 | 68.4 | 21.1 |
| relative standard deviation (SD/mean) | 9.9% | 19.7% | 32.5% | 63.5% | 24.7% |
| $1/\sigma^2$-weighted average | 0.22 | 4.7 | 0.8 | 88 | 79 |
| $1/\sigma^2$-weighted $\sigma$ of weighted average | 0.02 | 0.7 | 0.2 | 60 | 5 |

Table 3. Correlation coefficients for the AXUV-100G diode responsivity parameters of Table 1.

| | 130 eV responsivity | oxide thickness | carbon layer thickness | "dead" layer silicon thickness | dead layer collection efficiency |
|---|---|---|---|---|---|
| oxide thickness | -0.17 | 1.00 | 0.22 | 0.32 | 0.02 |
| carbon layer thickness | -0.38 | 0.22 | 1.00 | 0.48 | 0.49 |
| "dead" layer silicon thickness | -0.75 | 0.32 | 0.48 | 1.00 | 0.59 |
| dead layer collection efficiency | -0.23 | 0.02 | 0.49 | 0.59 | 1.00 |

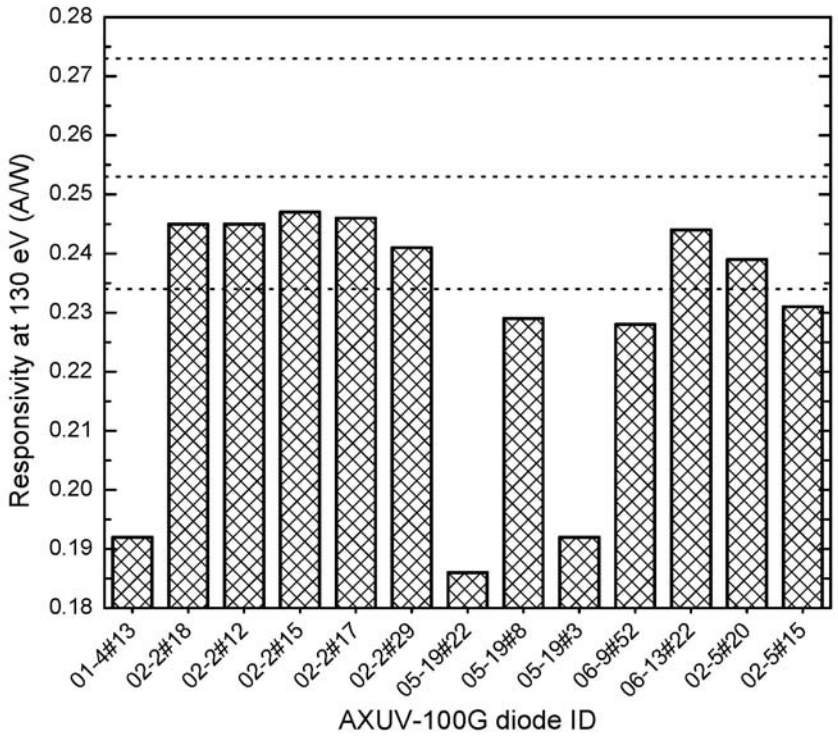


Fig. 4. Responsivity at 130 eV for the diodes under study (each carries 2-5% error associated with it). Reference lines are drawn for maximum possible responsivity, responsivity of dead-layer-free diode, and target performance responsivity as described in the text.

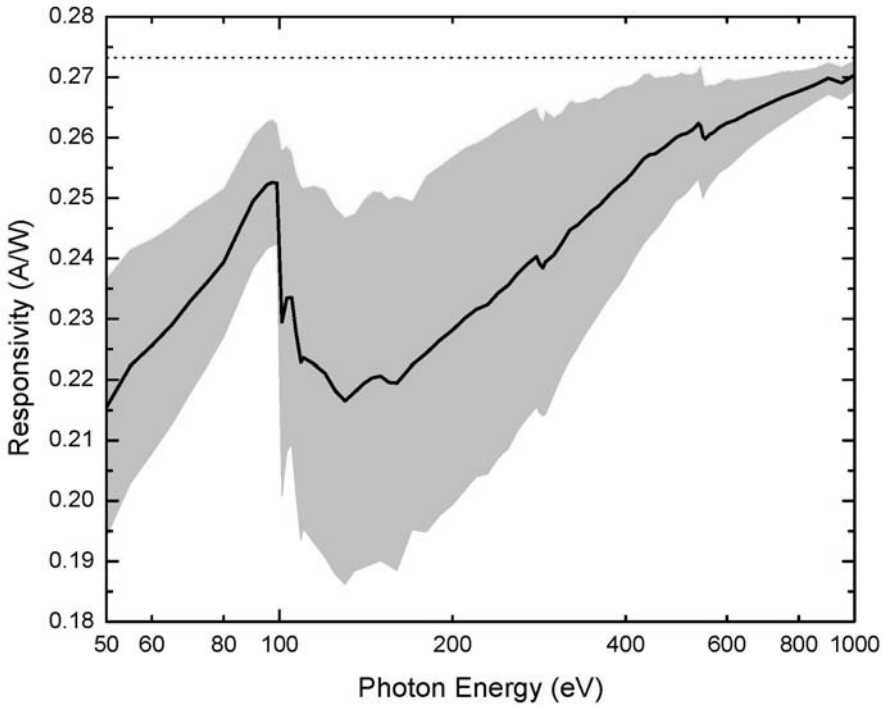


Fig. 5. "Typical" responsivity curve of AXUV-100G diodes in 50-1000 eV photon energy range, compiled from data of 13 diodes. The physical limit of S = 1/*w* is indicated as a dotted line.

### 3.5 Lifetime of individual photodiodes

Soft x-ray photon-induced damage of silicon photodiodes is not well understood. Some of the observed behavior includes localized damage under high flux, robustness against responsivity degradation with nitridation, and spontaneous "repair" and/or degradation of diode responsivity when illumination is removed[3, 4, 39]. Repair by annealing has also been observed. However, from our experience, annealing at room temperature may be as effective as annealing at 100 °C. Some diodes have also been found to spontaneously degrade under no illumination. This behavior is not understood, but luckily it is not common.

Typical lifetime for photodiodes in use at the NSLS U3c beamline is 1-2 years. The dose corresponds to roughly $10^9$ photons per second over a 0.02 $cm^2$ area, for roughly 100-500 hours per year, at energies ranging from 50 to 1000 eV. The performance metric for lifetime in use at the U3c beamline is 5% degradation of responsivity at any energy. Likewise, we have measured shunt resistance degradation over time, and found that it can drop by an order of magnitude or more. Typical lifetime for diodes starting at 200-500 MΩ shunt resistance and eventually giving more than 1 pA dark current in our environment is 1-2 years and corresponds to ~ 50-90% degradation in shunt resistance. Since the beamline end-chamber is kept at high vacuum ($10^{-7}$ Torr), carbon contamination is not suspected. Instead, soft x-ray illumination and/or spontaneous degradation of the diode structure is thought to limit the lifetime of silicon photodiodes.

This damage is not fully understood, but there are several methods available to investigate and/or mitigate the problem:

1. To characterize this damage, the stability test proposed in reference [4] is recommended. However, since that test is normally performed at 10.2 eV, additional tests at higher photon energies are desired (e.g. 130 eV). However, since the synchrotron is not a constant-output source, some means of normalizing to flux is desired which will not subject a reference detector to excessive dose.
2. Applying a known high flux to a localized area, and afterwards measuring responsivity across the surface of the diode may give clues about the relationship between shunt resistance and responsivity degradation.
3. Use of the IRD SXUV device has been recommended in the literature for environments of high flux [45]. This diode is not studied in the current paper but it is worth noting that this diode does not have the same simple device structure of the AXUV-100G. In addition to possible dead layer silicon, oxide, and carbon layers in the "window", this device is designed to also include a silicon-rich dead layer ("silicide", with metal such as Pt or Ti). Since this material is of unknown composition, it cannot readily be calibrated using the "self calibration" method. Study of this diode with respect to damage requires transfer calibration from another standard, plus dedicated illumination studies for verification of the literature result referenced. It will be useful to quantify the variability of those diodes as well.

## 4. SUMMARY

The use of silicon photodiodes for absolute, current-measurement radiometry in the soft x-ray range is described. Figures of merit for such detectors include shunt resistance, responsivity, silicon dead layer (matching), and damage threshold (lifetime). Responsivity of 13 diodes from 6 batches of AXUV-100G diodes has been reported; responsivity curves were measured and fit with a simple model in the soft x-ray range (50-1000 eV), revealing significant variability in window transmission and efficiency, peaking at ~25% total range at 130 eV photon energy. Consequently, the performance metric for this feature is 0.234 A/W at 130 eV which roughly corresponds to a maximum silicon dead layer of 50 nm (at 90% collection efficiency). Most, but not all diodes from a given batch were found to match each other in terms of responsivity within 2%. Shunt resistance varies by as much as 4 orders of magnitude among diodes even from the same batch. Our specification is 500 MΩ minimum. Both responsivity and shunt resistance are found to degrade over time and/or exposure to VUV illumination. Responsivity degradation is localized; lifetime is reached when localized responsivity falls by 5% or shunt resistance falls by 50%.

## 5. ACKNOWLEDGMENTS

The author wishes to thank Benjawan Kjornrattanawanich of NRL for assistance during collection of some of the data presented. Also the author would like to acknowledge valuable discussions with Frank Scholze of PTB, Rob Vest of NIST and John Seely of NRL regarding experience with the IRD AXUV diodes. This work is made possible with the support of National Security Technologies, LLC and the scientific staff of LLNL, LANL, and SNL which rely on calibrated x-ray detectors, notably the PRT management of the NSLS U3c and X8a beamlines [11].

## REFERENCES

1. R. Korde, C. Prince, D. Cunningham, et al., "Present Status of Radiometric Quality Silicon Photodiodes," Metrologia 40, S145-S149 (2003).
2. E. M. Gullikson, R. Korde, L. R. Canfield, et al., "Stable Silicon Photodiodes for Absolute Intensity Measurements in the VUV and Soft X-Ray Regions," J. Elec. Spec. Rel. Phen. 80, 313-316 (1996).
3. L. R. Canfield, in *Vacuum Ultraviolet Spectroscopy II*, edited by J. A. Samson and D. E. Ederer (Academic Press, San Diego, CA, 1998), pp. 117-138.
4. R. Korde, J. S. Cable and L. R. Canfield, "One Gigarad Passivating Nitrided Oxides for 100% Internal Quantum Efficiency Silicon Photodiodes," IEEE Trans. Nucl. Sci. 40(6), 1655-1659 (1993).
5. B. Kjornrattanawanich, R. Korde, C. N. Boyer, et al., "Temperature Dependence of the EUV Responsivity of Silicon Photodiode Detectors," IEEE Trans. Electron Devices 53(2), 218-223 (2006).
6. L. R. Canfield, R. E. Vest, R. Korde, et al., "Absolute Silicon Photodiodes for 160 nm to 254 nm Photons," Metrologia 35, 329-334 (1998).
7. IRD, "IRD Website," [http://www.ird-inc.com/].
8. M. L. Polignano, M. Alessandri, B. Crivelli, et al., "The Impact of the Nitridation Process on the Properties of the Si-SiO2 Interface," J. Non-Cryst. Solids 280, 39-47 (2001).
9. H. Yang, H. Niimi, Y. Wu, et al., "The Effects of Interfacial Suboxide Transition Regions on Direct Tunneling in Oxide and Stacked Oxide-Nitride Gate Dielectrics," Microelectronic Engineering 48, 307-310 (1999).
10. J. W. Keister, J. E. Rowe, J. J. Kolodziej, et al., "Structure of Ultrathin SiO2/Si(111) Interfaces Studied by Photoelectron Spectroscopy," J. Vac. Sci. Technol. A 17(4), 1250-1257 (1999).
11. J. Keister, "Website of NSLS Beamlines U3c and X8a," [http://www.bnl.gov/u3cx8a/].
12. NSLS, "NSLS Beamline U3C Web Page," [http://www.nsls.bnl.gov/beamlines/beamline.asp?blid=U3C].
13. NSLS, "NSLS Beamline X8A Web Page," [http://www.nsls.bnl.gov/beamlines/beamline.asp?blid=X8A].
14. R. J. Bartlett, W. J. Trela, F. D. Michaud, et al., "Characteristics and Performance of the Los Alamos VUV Beam Line At the NSLS," Nucl. Instr. Meth. A266, 199 (1988).
15. R. H. Day, R. L. Blake, G. L. Stradling, et al., "Los Alamos X-Ray Characterization Facilities for Plasma Diagnostics," SPIE Conference "X-ray Calibration, Techniques, Sources and Detectors" 689, 208 (1986).
16. F. C. Brown, J. P. Stott and S. L. Hulbert, "First Operation of an Extended Range Grasshopper Monochromator on the Aladdin Storage Ring," Nucl. Instr. Meth. A246, 278 (1986).
17. M. Krumrey and E. Tegeler, "Self-Calibration of Semiconductor Photodiodes in the Soft-X-Ray Region," Rev. Sci. Instrum. 63(1), 797 (1992).
18. M. Krumrey, E. Tegeler, R. Goebel, et al., "Self-Calibration of the Same Silicon Photodiode in the Visible and Soft-X-Ray Ranges," Rev. Sci. Instrum. 66(9), 4736 (1995).
19. F. Scholze, H. Rabus and G. Ulm, "Mean Energy Required to Produce an Electron-Hole Pair in Silicon for Photons of Energies Between 50 and 1500 eV," Journal of Applied Physics 84(5), 2926-2939 (1998).
20. B. L. Henke, E. M. Gullikson and J. C. Davis, "X-Ray Interactions: Photo Absorption, Scattering, Transmission, and Reflection At E = 50-30000 eV, Z = 1-92," Atomic Data and Nucl. Data Tables 54(2), 181 (1993).
21. CXRO, "X-Ray Interactions With Matter Web Page," [http://henke.lbl.gov/optical_constants/].
22. J. Rife and J. Osantowski, "Extreme Ultraviolet Optical Properties of Two SiO2 Based Low-Expansion Materials," J. Opt. Soc. Am. 70, 1513 (1980).
23. K. M. Campbell, F. A. Weber, E. L. Dewald, et al., "Omega Dante Soft X-Ray Power Diagnostic Component Calibration At the National Synchrotron Light Source," Rev. Sci. Instrum. 75, 3768 (2004).
24. E. L. Dewald, K. M. Campbell, R. E. Turner, et al., "Dante Soft X-Ray Power Diagnostic for National Ignition Facility," Rev. Sci. Instrum. 75, 3759 (2004).

25. R. J. Leeper, G. A. Chandler, G. W. Cooper, et al., "Target Diagnostic System for the National Ignition Facility," Rev. Sci. Instrum. 68, 868 (1997).
26. M. E. Cuneo, R. A. Vesey, J. L. Porter, et al., "Development and Characterization of a Z-Pinch-Driven Hohlraum High-Yield Inertial Confinement Fusion Target Concept," Physics of Plasmas 8(5), 2257-2267 (2001).
27. K. L. Baker, J. L. Porter, L. E. Ruggles, et al., "Soft X-Ray Measurements of Z-Pinch-Driven Vacuum Hohlraums," Appl. Phys. Lett. 75(6), 775-777 (1999).
28. J. J. MacFarlane, J. E. Bailey, G. A. Chandler, et al., "X-Ray Absorption Spectroscopy Measurements of Thin Foil Heating by Z-Pinch Radiation," Phys. Rev. E 66, 046416 (2002).
29. G. A. Chandler, C. Deeney, M. Cuneo, et al., "Filtered X-Ray Diode Diagnostics Fielded on the Z Accelerator for Source Power Measurements," Rev. Sci. Instrum. 70(1), 561-565 (1999).
30. C. Sorce, J. Schein, F. Weber, et al., "Soft X-Ray Power Diagnostic Improvements At the Omega Laser Facility," Rev. Sci. Instrum. 77, 10E518 (2006).
31. G. A. Rochau, J. E. Bailey, G. A. Chandler, et al., "Energy Dependent Sensitivity of Microchannel Plate Detectors," Rev. Sci. Instrum. 77, 10E323 (2006).
32. L. R. Canfield, R. Vest, T. N. Woods, et al., "Silicon Photodiodes with Integrated Thin Film Filters for Selective Bandpasses in the Extreme Ultraviolet," SPIE Conference "Ultraviolet Technology V" 2282, 31-38 (1994).
33. J. F. Seely, R. Korde, F. Hanser, et al., "Characterization of Silicon Photodiode Detectors with Multilayer Filter Coatings for 17-150 Å," SPIE Conference "Ultraviolet and X-ray Detection, Spectroscopy and Polarimetry III" 3764 (1999).
34. B. Kjornrattanawanich, J. Seely, R. Korde, et al., "Temperature and Polarization Performance of EUV Silicon Photodiodes," Synchrotron Radiation Instrumentation: Eighth International Conference CP705, 1005-1008 (2004).
35. P. S. Shaw, K. R. Lykke, R. Gupta, et al., "Ultraviolet Radiometry with Synchrotron Radiation and Cryogentic Radiometry," Applied Optics 38(1), 18-28 (1999).
36. H. Rabus, V. Persch and G. Ulm, "Synchrotron-Radiation-Operated Cryogenic Electrical-Substitution Radiometer As the High-Accuracy Primary Detector Standard in the Ultraviolet, Vacuum-Ultraviolet, and Soft-X-Ray Spectral Ranges," Applied Optics 36(22), 5421-5440 (1997).
37. F. Scholze, J. Tümmler and G. Ulm, "High-Accuracy Radiometry in the EUV Range At the PTB Soft X-Ray Beamline," Metrologia 40, S224-S228 (2003).
38. F. Scholze, G. Brandt, P. Müller, et al., "High-Accuracy Detector Calibration for EUV Metrology At PTB," SPIE conference "Emerging Lithographic Technologies VI" 4688, 680-689 (2002).
39. L. R. Canfield, J. Kerner and R. Korde, "Stability and Quantum Efficiency Performance of Silicon Photodiode Detectors in the Far Ultraviolet," Applied Optics 28(18), 3940-3943 (1989).
40. T. Saito and H. Onuki, "Detector Calibration in the Wavelength Region 10 nm to 100 nm Based on a Windowless Rare Gas Ionization Chamber," Metrologia 32, 525-529 (1996).
41. R. H. Pehl, F. S. Goulding, D. A. Landis, et al., "Accurate Determination of the Ionization Energy in Semiconductor Detectors," Nuclear Instruments and Methods 59, 45-55 (1968).
42. M. D. Ulrich, J. E. Rowe, J. W. Keister, et al., "Comparison of Ultrathin SiO2/Si(100) and SiO2/Si(111) Interface From Soft X-Ray Photoelectron Spectroscopy," J. Vac. Sci. Technol. B 24(4), 2132-2137 (2006).
43. J. F. Seely, "Responsivity Model for a Silicon Photodiode in the Extreme Ultraviolet," SPIE conference "Instrumentation for UV/EUV Astronomy and Solar Missions" 4139 (2000).
44. R. Hartmann, P. Lechner, L. Strüder, et al., "The Radiation Entrance Window of Pn Junction Detectors," Metrologia 32, 491-494 (1995).
45. F. Scholze, R. Klein and T. Bock, "Irradiation Stability of Silicon Photodiodes for Extreme-Ultraviolet Radiation," Applied Optics 42(28), 5621-5626 (2003).